NAVY ENVIRONMENTALLY SAFE SHIPS PROGRAM

EXPERIMENTAL STUDIES OF RADIAL WAVE THERMOACOUSTIC ENGINES

ANNUAL REPORT

Grant #: N00014-93-1-1125

Submitted to:

Office of Naval Research
Physics Division ONR 331
800 North Quincy
Arlington, Virginia 22217-5660

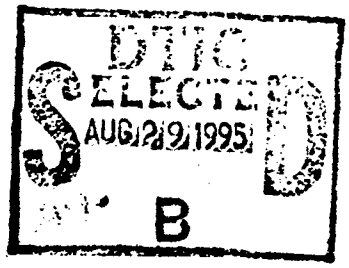

by:

Richard Raspet, Henry E. Bass and Jay A. Lightfoot
National Center for Physical Acoustics
The University of Mississippi
University, Mississippi 38677

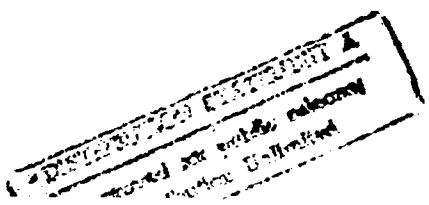

NCPA Report RR0795-01

NAVY ENVIRONMENTALLY SAFE
SHIPS PROGRAM

EXPERIMENTAL STUDIES OF RADIAL WAVE
THERMOACOUSTIC ENGINES

ANNUAL REPORT

The Jamie Whitten National Center for Physical Acoustics

The
University of Mississippi

REPORT DOCUMENTATION PAGE

Form Approved
OMB No. 0704-0188

1. AGENCY USE ONLY (Leave blank)	2. REPORT DATE	3. REPORT TYPE AND DATES COVERED
	15 July 1995	Annual 01 June 94 - 31 May 95

4. TITLE AND SUBTITLE

Experimental Studies of Radial Wave Thermoacoustic Engines

5. FUNDING NUMBERS

PE 61153N
G N00014-93-1-1125
TA 3126973ess01

6. AUTHOR(S)

Richard Raspet, Henry E. Bass and Jay A. Lightfoot

7. PERFORMING ORGANIZATION NAME(S) AND ADDRESS(ES)

National Center for Physical Acoustics
The University of Mississippi
University, MS 38677

8. PERFORMING ORGANIZATION REPORT NUMBER

RR0795-01

9. SPONSORING/MONITORING AGENCY NAME(S) AND ADDRESS(ES)

Office of Naval Research
ONR 331
800 North Quincy Street
Arlington, VA 22217-5660

10. SPONSORING/MONITORING AGENCY REPORT NUMBER

11. SUPPLEMENTARY NOTES

12a. DISTRIBUTION/AVAILABILITY STATEMENT

Approved for public release: Distribution unlimited

12b. DISTRIBUTION CODE

13. ABSTRACT (Maximum 200 words)

The horizontal plate prime mover has been constructed and reported at the fall meeting of the ASA in Austin, TX. The analysis of horizontal plate thermoacoustic engines has been completed and submitted for publication in JASA and a theoretical comparison of plane and radial wave thermoacoustic engines was reported in Austin. Analysis of vertical plate thermoacoustic engines has recently been completed and a manuscript is being reviewed. Preliminary vertical plate prime mover results were reported at the spirng meeting of the ASA in Washington, DC.

14. SUBJECT TERMS

Thermoacoustics, Prime mover, Horizontal and vertical plate

15. NUMBER OF PAGES

28

16. PRICE CODE

TABLE OF CONTENTS

Page

BRIEF DESCRIPTION OF ACCOMPLISHMENTS 1

I. Radial Prime Mover Prototype 1

II. Horizontal Plate Thermoacoustic Engines 3

III. Thermoacoustic Engines with Varying Plate Separation 3

A. "Sloped" engine wave equation 4
B. Pressure and specific acoustic impedance differential equations 6
C. Prime mover results 7
D. Plane wave results 8
E. Radial wave results 10

IV. Thermoacoustic Helmholtz Resonator 12

V. References 13

PUBLICATION/PATENTS/PRESENTATION/HONORS REPORT 27

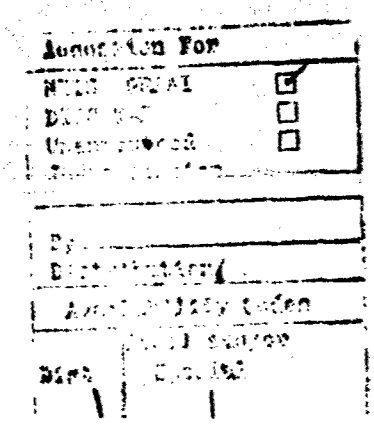

EXPERIMENTAL STUDIES OF RADIAL WAVE THERMOACOUSTIC ENGINES

ANNUAL REPORT

BRIEF DESCRIPTION OF ACCOMPLISHMENTS

The horizontal plate prime mover has been constructed in collaboration with Dr. Arnott at the University of Nevada at Reno, and was reported at the fall meeting of the Acoustical Society of America in Austin, Texas.[1] The analysis of horizontal plate thermoacoustic engines has been completed and submitted for publication in the Journal of the Acoustical Society of America,[2] and a theoretical comparison of plane and radial wave thermoacoustic engines was reported in Austin.[3] Report was also made at Austin of a previously described Helmholtz resonator prime mover.[4] Analysis of vertical plate thermoacoustic engines has recently been completed and a manuscript is being reviewed. Preliminary vertical plate prime mover results were reported at the spring meeting of the Acoustical Society of America in Washington, DC.[5]

I. Radial Prime Mover Prototype

A schematic of the radial mode prime mover stack which has been constructed is given in Fig. 1 and the resonator is shown in Fig. 2. The system is optimized for a gas mixture of 60% Helium and 40% Argon at a pressure of 1 atm with an operating frequency of about 1.8 kHz. The cylindrical resonator is 12 inches in diameter and 4 inches high. The outer ring is aluminum and the top and bottom plates are stainless steel. The stack is made of a mica composite with an outer diameter of 10.346 inches and an inner diameter of 9.362 inches. The theoretical prediction for the temperature difference between the hot and cold sides of the stack at which the quality factor goes to infinity (onset temperature difference) is upwards of 200 K, depending on the heat exchanger design.

Based upon some plane wave prime mover experiments at the University of Mississippi which showed that cooling the resonator near the end [illegible] a heat exchanger

next to the stack, the initial cold heat exchanger design consisted of copper tubing to cool the top and bottom plates, and brass screen and copper tubing to function as a simple heat exchanger. The predicted onset temperature difference was about 200 K. This design proved to be oversimplified. A small increase in the quality factor of the system was measured, but the maximum temperature difference achieved was only about 100 K. A more conventional vertical plate copper heat exchanger was constructed by Dr. Arnott. The predicted onset temperature was about 275 K. Although the capacity for heat exchange is much greater than that of the former heat exchanger, the attenuation is also much greater as is evidenced by a significantly larger onset temperature. The greatest temperature difference achieved was about 150 K.

The hot side is heated by nichrome wire, and there appears to be no problem supplying enough heat in this way. The problem we are having in maintaining this large temperature difference across a short distance is one of cooling capability. Several potential problems have been investigated: thermal conduction across the stack through the top and bottom plates of the resonator and radiation from the nichrome wire through the stack. When the heater–stack–cold heat exchanger system is removed from the casing and covered with insulation top and bottom (effectively removing thermal conduction through the top and bottom plates), the largest temperature difference achieved is 180 K. Therefore, cutting down heat conducted across the resonator plates can increase ΔT by up to 30 K. A brass screen was then wrapped around the outside of the stack in order to reduce the amount of radiation transmitted across the stack to the cold heat exchanger, while leaving the system out of the casing and insulated on top and bottom. The largest temperature difference achieved was 170 K. The 10 K difference between the screened result and the non-screened result is probably due to thermocouple placement. Therefore, it appears that radiation is not significantly contributing to the heating of the cold heat exchanger.

Since the trouble is due to a difficulty in establishing the necessary temperature gradient, an attempt is being made to reduce this quantity. Calculations show that a stack identical to the present one placed in a resonator whose diameter is 58 inches, thus shifting the stack from

outside the pressure node to inside the pressure node, will require a ΔT of 65 K for air at atmospheric pressure. For this small ΔT, the present cold heat exchanger can be used as the new hot heat exchanger. It remains only to construct a larger resonator and a new cold heat exchanger. This will be accomplished shortly.

II. Horizontal Plate Thermoacoustic Engines

A paper has been submitted describing the full theory for horizontal plate thermoacoustic engines, including application to thermoacoustically enhanced photoacoustic spectroscopy and a theoretical comparison of plane and radial wave prime movers and refrigerators.[2] Dr. Arnott's report gives a detailed description of this work.

III. Thermoacoustic Engines with Varying Plate Separation

Swift showed for parallel plate thermoacoustic engines that the thermoacoustic effect is optimized when the plate spacing is roughly twice the thermal penetration depth.[6] Bennett realized that varying the plate spacing from the cold side to the hot side of a thermoacoustic engine had two possible benefits (pp. 159-162 of Ref. 7). First, it allows optimal thermal contact between the fluid and the engine wall to be closely approximated throughout the engine,[5] since the thermal penetration depth varies with temperature. Second, it can reduce acoustic losses by matching impedances at both interfaces of the engine as in a loudspeaker horn.[8] Bennett formulated an analytic solution to the problem by adopting Swift's parallel plate wave equation (Eq. 54 of Ref. 6) and allowing for a constant slope between successive plates (pp. 131-132 of Ref. 7).

Analyzing Bennett's work for application to radial wave thermoacoustic engines, it became

thermoacoustic engines having a varying plate separation. Rott correctly approached this type of

[5] In order to exactly achieve optimal spacing throughout the engine, a nonlinear slope would have to be assumed since the temperature distribution in the engine is not linear (p. 162 of Ref. 7).

problem while considering sound propagation in tubes with variable cross-section by introducing the changing tube cross-sectional area into the wave equation,[9] as in Webster's horn equation (Eq. 7–8.5 of Ref. 10). The theory of sloped engine thermoacoustics is described below and its effect in prime movers is numerically quantified.

A. "Sloped" engine wave equation

The thermoacoustic wave equation for the parallel plate thermoacoustic engine of Fig. 3 is given by Eq. 28 of Ref. 11 to be

$$\frac{\rho_0}{F(\lambda)} \frac{d}{dr}\left[\frac{F(\lambda)}{\rho_0}\frac{dp_1}{dr}\right] + 2a(\lambda, \lambda_T)\frac{dp_1}{dr} + k^2(\lambda, \lambda_T)\, p_1 = 0 \,, \tag{1}$$

where

$$a(\lambda, \lambda_T) = \frac{\beta}{2}\left(\frac{F(\lambda_T)/F(\lambda) - 1}{1-\sigma}\right)\frac{dT_0}{dr} \,, \tag{2}$$

$$k^2(\lambda, \lambda_T) = \frac{\omega^2}{c^2 F(\lambda)}\left[\gamma - (\gamma - 1) F(\lambda_T)\right] \,, \tag{3}$$

$$F(\xi) = 1 - (2/\xi\sqrt{-i}) \tanh(\sqrt{-i}\xi/2) \,. \tag{4}$$

γ is the ratio of fluid specific heats, $\rho_o(r)$ is the ambient fluid density, c is the speed of sound in the fluid, ω is the oscillatory angular frequency of the acoustic variables, $p_1(r)$ is the acoustic pressure, β is the coefficient of thermal expansion of the fluid, σ is the Prandtl number of the fluid, $T_0(r)$ is the mean fluid temperature.

$$\lambda = \sqrt{2}\gamma/\delta_\kappa \,, \tag{5}$$

$$\lambda_T = \lambda\sqrt{\sigma} = \sqrt{2}y/\delta_\kappa \ , \qquad (6)$$

δ_κ (δ_ν) is the thermal (viscous) penetration depth in the fluid, and y is the plate separation.

Figure 4 shows a thermoacoustic engine with a constant slope between successive plates. Bennett accounted for a sloped engine by replacing y with $y\,(r)$ in the parallel plate wave equation (Eq. 1), where

$$y\,(r) = y_0 + sr \ , \qquad (7)$$

y_0 is the plate separation at the cold (left) side of the engine, $s = y_L - y_0 / L$ is the slope of the plates relative to each other, L is the engine or stack length, $y_L = y\,(L)$ is the plate separation at the hot (right) side of the engine, and r is the distance from the cold (left) side of the engine.

Adopting Bennett's method of allowing for a constant slope between successive plates, λ and λ_T in Eq. 1 are now position dependent quantities since y_0 has been replaced by $y\,(r)$. However, examination of Rott's work with tubes of varying cross-section[9] reveals the need for a fundamental change in Eq. 1 for sloped engines — allowing for area changes within individual pores in the stack as in Webster's horn equation — in addition to making λ and λ_T position dependent. The correct wave equation for stacked plate thermoacoustic engines with varying plate spacing is

$$\frac{\rho_0}{A_p(r)\,F\,(\lambda)}\,\frac{d}{dr}\left[\frac{A_p(r)\,F\,(\lambda)}{\rho_0}\,\frac{dp_1}{dr}\right] + 2\alpha\,(\lambda, \lambda_T)\,\frac{dp_1}{dr} + k^2(\lambda, \lambda_T)p_1 = 0 \ , \qquad (8)$$

where $A_p(r)$ is the cross-sectional area between two plates at a location r (or the pore cross-sectional area) in the engine and y is replaced with $y\,(r)$ from Eq. 7 in λ and λ_T. The radial thermoacoustic wave equation can be derived with $A_p(r)$ being the radial pore cross-sectional area and is identical to previous results.[2,6]

B. Pressure and specific acoustic impedance differential equations

The derivation to follow is analogous to that of Ref. 11, with r dependence showing up in some previously constant terms due to the changing cross-sectional area between the plates. Define as a pore the space between two plates. Let $v_r(r)$ be the average particle velocity for a particular pore cross-section, n the total number of pores in the engine, $A_{res}(r)$ the resonator cross-sectional area at r, $Ap(r)$ the cross-sectional area of a pore at r, V_{rb} the bulk velocity for the resonator at r, and $\Omega(r)$ the porosity or the ratio of open area to total area in the engine at r. Volume velocity is $A_{res}(r)V_{rb} = nAp(r)v_r(r)$, but $\Omega(r) = nAp(r)/A_{res}(r)$; therefore, $v_r(r) = V_{rb}/\Omega(r)$.

The equation of motion for the fluid in a pore is given in Eq. 13 of Ref 11 as $i\omega\rho_0 v_r(r) = F(\lambda)(dp_1/dr)$ which, with the expression for $v_r(r)$ above, can be written as

$$i\omega\rho_0 \frac{V_{rb}}{\Omega(r)} = F(\lambda)\frac{dp_1}{dr} \quad . \tag{9}$$

With the definition of specific acoustic impedance

$$Z(r) = \frac{p_1(r)}{V_{rb}(r)} \quad , \tag{10}$$

the first order differential equation for pressure is found from Eqs. 9 and 10 to be

$$\frac{dp_1(r)}{dr} = ik(\lambda, \lambda_T) Z_{int}(r) \frac{p_1(r)}{Z(r)} \quad , \tag{11}$$

where

$$Z_{int} = \frac{\rho_0 \omega}{\Omega(r) F(\lambda) k(\lambda, \lambda_T)} . \qquad (12)$$

The impedance equation is derived by inserting Eqs. 9, 10, and 12 into Eq. 8, with the result given by

$$\frac{dZ(r)}{dr} = ik(\lambda,\lambda_T) Z_{int}(r) \left[1 - \frac{Z^2(r)}{Z_{int}^2(r)}\right] + \left\{2\alpha(\lambda,\lambda_T) + \frac{\Omega(r)}{A_p(r)} \frac{d}{dr}\left[\frac{A_p(r)}{\Omega(r)}\right]\right\} Z(r) . \qquad (13)$$

Given the definition of $\Omega(r)$ above, Eq. 13 can also be written

$$\frac{dZ(r)}{dr} = ik(\lambda,\lambda_T) Z_{int}(r) \left[1 - \frac{Z^2(r)}{Z_{int}^2(r)}\right] + \left\{2\alpha(\lambda,\lambda_T) + \frac{1}{A_{res}(r)} \frac{d}{dr}\left[A_{res}(r)\right]\right\} Z(r) . \qquad (14)$$

C. Prime mover results

The heat exchanger temperature difference (*onset temperature*) at which $Q \rightarrow \infty$ for a given ambient heat exchanger temperature, where Q is the resonator quality factor, can be determined by integration of Eqs. 11 and 13. Numerical integration of similar equations is described in Ref. 2 for radial wave prime movers and in Ref. 11 for plane wave prime movers. The integration for sloped stack, plane and radial wave prime movers was achieved by adapting the solution described in Refs. 2 and 11 such that the varying plate spacing, cross-sectional area, and porosity were included.

Arnott *et al* showed that for parallel plate thermoacoustic engines the optimal plate spacing occurs when $\lambda_T = 3.2$ (Ref. 11), which corresponds to a plate separation of 2.26 δ_K (this is the plate separation at the hot end of the engine, since $\lambda_T = 3.2$ corresponds to a greater plate separation at the hot end than at the cold end). δ_K is smaller at the cold side of an engine, so for an optimally spaced parallel plate engine the plate separation on the cold side is greater than the plate separation which would achieve the best thermal contact. Define the *slope ratio* as the ratio

of the actual engine slope s to the slope which gives optimal thermal contact, where optimal thermal contact slope is determined by setting $\lambda_T = 3.2$ at the hot and cold ends of the engine. Positive (negative) *slope ratio* corresponds to a wider plate spacing at the hot (cold) side of the engine.

D. Plane wave results

Fig. 5 shows numerical calculations of ΔT, the onset temperature difference, as a function of *slope ratio* for the prime mover described in Table 1. The resonator cross-section is assumed to be square and the resonator length is held constant. The integration is initially run for zero slope to determine the optimal plate spacing for a parallel plate engine. This value is then assigned to y_0 at the cold side of the engine. As the slope is changed, the plate spacing at the hot side of the engine, y_L, changes; which requires one cross-sectional dimension of the tube on the hot side of the engine to vary due to the spreading of the engine (the other tube dimension is also varied to maintain a square geometry). Porosities of the heat exchangers on the hot and cold sides are held constant at all times. The process is then repeated for different values of y_0 to determine the lowest onset temperature achievable.

In Fig. 5, curve *a* provides the best thermal contact between the fluid and the solid at the cold side. If thermal contact were the dominant factor in decreasing ΔT, one would expect curve *a* with *slope ratio* = 1 to produce the lowest possible ΔT. It is obvious that this is not the case, since for curve *a* alone the lowest ΔT occurs when *slope ratio* ≈ 2.5. In addition, curves *b*, *c*, *d*, and *e*, which have plate spacings greater than 2.26 δ_κ, have much lower ΔTs than curve *a*. The solid dots represent the minima of curves *a-e* and additional data sets with different values of y_0. The lowest ΔT achievable for the parallel plate engine (curve *c* with *slope ratio* = 0) is about 137.5° C, while the overall minima (curve *d* with *slope ratio* ≈ 7.8) is about 131° C, so a carefully spaced and sloped engine decreases the onset temperature for this system by approximately 6.5° C. There are two additional things to note. First, curve *d*, which gives the lowest ΔT, has a wider plate spacing at all points than the lowest ΔT parallel plate spacing. Second, the *slope*

ratio which gives the lowest ΔT in curve *d* is large, so a smaller fraction of the fluid is in good thermal contact with the solid (see Fig. 6 for a physical picture). The above observations lead one to conclude that there is a trade-off between reducing acoustic losses via impedance matching using sloped stacks (and thus changing the resonator cross-section on the hot end) and having the fluid in good thermal contact with the solid, with impedance matching being the dominant quantity for reducing the onset temperature.

TABLE 1. Sloped stack plane wave prime mover specifications. "var" denotes quantities which vary with engine slope. Ambient temperature is 239 K, ambient pressure is 200 kPa, and the fluid is Helium.

Specification	Open Tube	Open Tube	Cold HX	Engine	Hot HX	Open Tube	Open Tube
Length (cm)	123.0	5.0	2.0	6.0	2.0	5.0	17.0
Height (cm)	10.0	10.0	10.0	var	var	var	10.0
Width (cm)	10.0	10.0	10.0	var	var	var	10.0
Left Side Porosity	1.0	10.0	0.640	var	0.640	1.0	1.0
Right Side Porosity	1.0	1.0	0.640	var	0.640	1.0	1.0
Plate Thickness (mm)			0.600	0.457	0.600		
Plate Material			copper	mica	copper		

An attempt has been made to hold as many parameters constant as possible in order to isolate the effects of thermal contact and impedance matching. One of these parameters is the location of the engine in the standing wave. This location was chosen such that it produced a minimum ΔT for the parallel plate configuration. When this parameter is allowed to change,

even lower ΔTs are achieved using a sloped engine by sliding the heat exchanger – stack – heat exchanger system in the direction of the hot end and allowing the plate spacing and slope to increase beyond that which gives the lowest ΔT in the original location.

E. Radial wave results

Radial wave prime movers with "washer" style stacks have been investigated,[2] and are related to the plane wave parallel plate engines in the sense that both have a constant plate spacing from one side of the stack to the other. Fig. 7 is a schematic of the two radial stacks being compared. ΔT for two different radial wave prime movers with varying plate spacing have been plotted against the *slope ratio* and have been compared with the ΔT achievable using a "washer" style engine in the same resonators and with the same radial lengths and locations. Note that the actual slope between the plates in the radial system is completely determined by the number of plates, the plate thickness, and the radial location of the stack; therefore, it is impossible to choose a cold side spacing and sweep through a range of slopes.

The first radial system considered is a scaled version of the plane wave system described in Table 1 such that the resonant frequency of the radial resonator is the same as that of the plane resonator (314 Hz). The dimensions and specifications of the 314 Hz radial vertical stack system are given in Table 2, and Fig. 8 shows ΔT as a function of *slope ratio*. The minimum ΔT calculated for the vertical plate prime mover is 169.0°C compared to a low of 161.1°C for the "washer" style engine. The second radial system considered is a model presently being worked on which has an operating frequency of about 1.37 kHz. The dimensions and specifications of the 1.37 kHz radial vertical stack system are given in Table 3, and Fig. 9 shows ΔT as a function of *slope ratio*. The minimum ΔT calculated for the vertical plate prime mover is 253.9°C compared to a low of 255.4°C for the "washer" style engine.

In both of the radial systems considered, the advantage of having a vertical "sloped" engine rather than a "washer" style engine is very small. Examination of Figs. 8 and 9 shows that radial sloped engines are confined to extremely low *slope ratios*, more than a factor of ten lower than

the *slope ratio* value which gives a minimum ΔT for the plane wave engine of Table 1. This means that the spacing in the radial vertical engines considered is only slightly different than the spacing in the comparable "washer" style engines. A higher *slope ratio* is achievable by decreasing the radial distance of the engine from the center, but this would tend to move the engine from outside the pressure node to inside the pressure node, radially reversing the relative locations of the hot and cold sides of the engine and causing the increasing slope to be in the wrong direction. Therefore, the small advantage gained by a carefully spaced, vertical plate, radial prime mover over a "washer" style prime mover is not worth any extra trouble which might be necessary in construction of such an engine. It had been hoped that the variation in plate spacing intrinsic to the radial vertical engine (sloped) geometry would be advantageous; however, due to decreased control of the slope and plate spacing combination, very little change in ΔT is predicted between the radial vertical engine and the radial "washer" style (parallel plate) engine.

TABLE 2. 314 Hz radial prime mover specifications. "var" denotes quantities which vary with engine slope. Ambient temperature is 293 K, ambient pressure is 200 kPa, and the fluid is Helium. Lengths are radial distances (i.e. there are 162 cm between the center of the resonator and the inside of the cold heat exchanger.

Specification	Open Tube	Cold HX	Engine	Hot HX	Open Tube
Length (cm)	162.0	2.0	7.0	2.0	22.0
Height (cm)	5.0	5.0	5.0	5.0	5.0
Porosity	1.0	0.640	var	0.640	1.0
Plate Thickness (mm)		0.000	0.457	0.000	
Plate Material		copper	mica	copper	

TABLE 3. 1.37 kHz radial prime mover specifications. "var" denotes quantities which vary with engine slope. Ambient temperature is 293 K, ambient pressure is 1 atm, and the fluid is a 50% Helium 40% Argon mixture. Lengths are radial distances (i.e. there are 10.62 cm between the center of the resonator and the inside of the cold heat exchanger.

Specification	Open Tube	Cold HX	Engine	Hot HX	Open Tube
Length (cm)	10.62	1.27	1.25	0.1	2.0
Height (cm)	10.16	10.16	10.16	10.16	10.16
Porosity	1.0	0.450	var	0.70	1.0
Plate Thickness (mm)		1.034	0.1524	1.0	
Plate Material		copper	mica	copper	

IV. Thermoacoustic Helmholtz Resonator

The construction of the thermoacoustically driven Helmholtz resonator of Fig. 10 was described in last year's report. The advantage of this type of prime mover is that it is a *compact*, low-frequency sound source. The operating frequency of this small prime mover is about 220 Hz. Experiments were performed using a conventional copper fin cold heat exchanger and using a section of cooled open tube. Three interesting things were found. First, the optimal location of the heat exchanger – stack – heat exchanger system (the location which gives the lowest ΔT) is such that the first obstruction to air flow occurs at the point where a uniform velocity is achieved in the body of the resonator. This occurs closer to the top for the cold open ring than for the copper fin heat exchanger, since for the open ring the first obstruction is the stack itself. Figures 11 and 12 show the power dissipated in the hot heat exchanger [illegible] locations with a cold heat exchanger and with open tube cooling. Second, it is seen from Figures 11 and 12 that the open tube cooling cuts down acoustic losses and requires less power to be delivered to the nichrome wire heater for onset to occur. Third, in a test of optimal orientation, it was found that having the neck of the resonator facing up, so that convection helps to heat the

hot side of the stack, requires a much lower power to be supplied to the nichrome wire heater for onset (when $Q \rightarrow \infty$) than when the neck is facing down (see Fig. 13).

Another accidental but interesting finding was that the radial prime mover described in the previous section can operate as a thermoacoustically driven Helmholtz resonator. When the temperature difference was built up across the stack and the microphone port was removed, a weak 106 Hz tone (which corresponds very nicely to the predicted Helmholtz resonance for this resonator) was heard.

V. References

1. J. A. Lightfoot, W. P. Arnott, R. Raspet and H. E. Bass, "Design of a radial mode thermoacoustic prime mover and experimental observations," J. Acoust. Soc. Am. 96, 3221 (1994).

2. W. P. Arnott, J. A. Lightfoot, R. Raspet and H. Moosmüller, "Radial wave thermoacoustic engines: Theory and examples for refrigerators, prime movers, and high-gain narrow-bandwidth photoacoustic spectrometers," (in preparation).

3. W. P. Arnott, J. Lightfoot, R. Raspet and H. E. Bass, "Radial versus plane wave thermoacoustic engines: Which is best?" J. Acoust. Soc. Am. 96, 3221 (1994).

4. R. Raspet, J. A. Lightfoot, J. R. Belcher and H. E. Bass, "Thermoacoustic sound source in the Helmholtz limit," J. Acoust. Soc. Am. 96, 3221 (1994).

5. J. A. Lightfoot, Richard Raspet, H. E. Bass and W. Patrick Arnott, "Plane and radial wave thermoacoustic engines with variable plate spacing," J. Acoust. Soc. Am. 97, 3410 (1995).

6. G. W. Swift, "Thermoacoustic engines," J. Acoust. Soc. Am. 84, 1145-1180 (1988).

7. Bennett, "Active cooling for downhole instrumentation: A miniature thermoacoustic refrigerator," dissertation from the University of New Mexico (1991).

8. D. E. Hall, *Basic Acoustics*, (John Wiley and Sons, Inc., New York, 1986) 286-289.

9. N. Rott and G. Zouzoulas, "Thermally driven acoustic oscillations, part IV: Tubes with variable cross-section," J. Appl. Math. and Phys. 27, 197-224 (1976).

10. A. D. Pierce, *Acoustics: An Introduction to Its Physical Principles and Applications*, (American Institute of Physics, New York, 1989).

11. W. P. Arnott, H. E. Bass, and R. Raspet, "General formulation of thermoacoustics for stacks having arbitrary shaped pore cross sections," J. Acoust. Soc. Am. 90, 3228-3237 (1991).

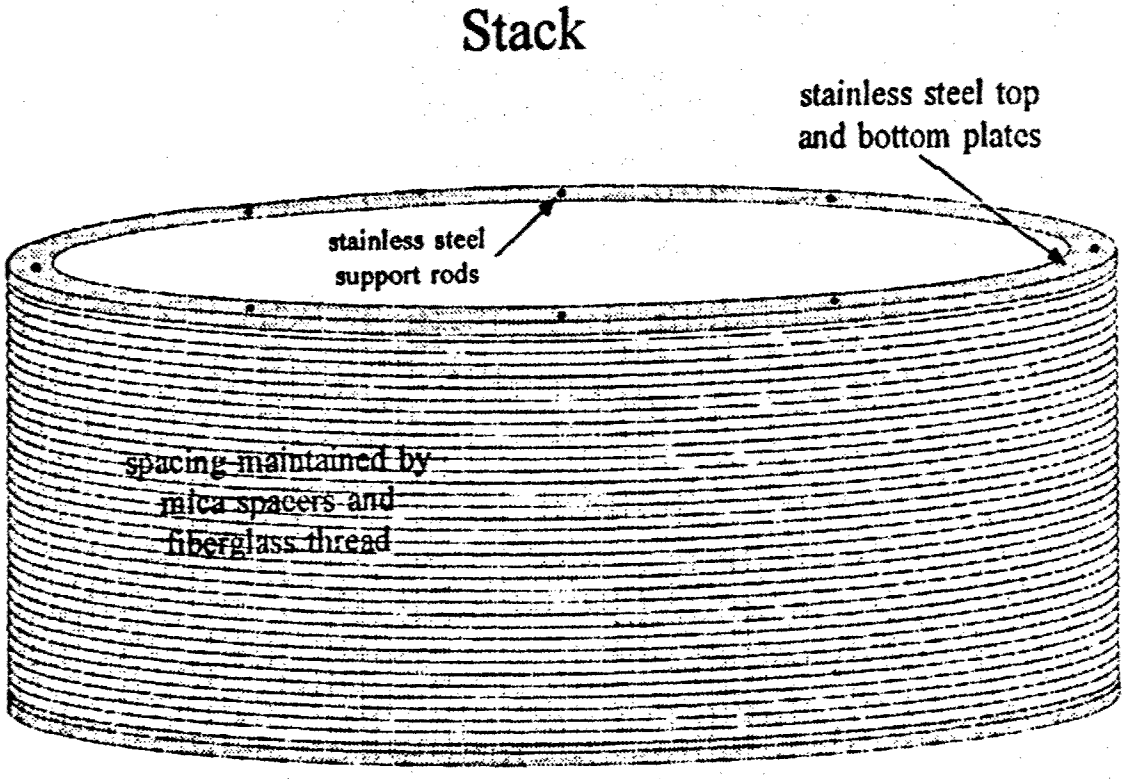

Mica Stack	Mica Spacers	Steel Plates
o.d. = 10.346 in.	*o.d. = 0.253 in.*	*o.d. = 10.346 in.*
i.d. = 9.362 in.	*i.d. = 0.120 in.*	*i.d. = 9.362 in.*
thickness = 0.006 in.	*thickness = 0.015 in.*	*thickness 0.063 in.*

radial stack length = 0.492 in. = 1.25 cm
stack height = 4 in.
# of mica plates = 177

Figure 1: Radial mode horizontal plate stack constructed at the University of Mississippi

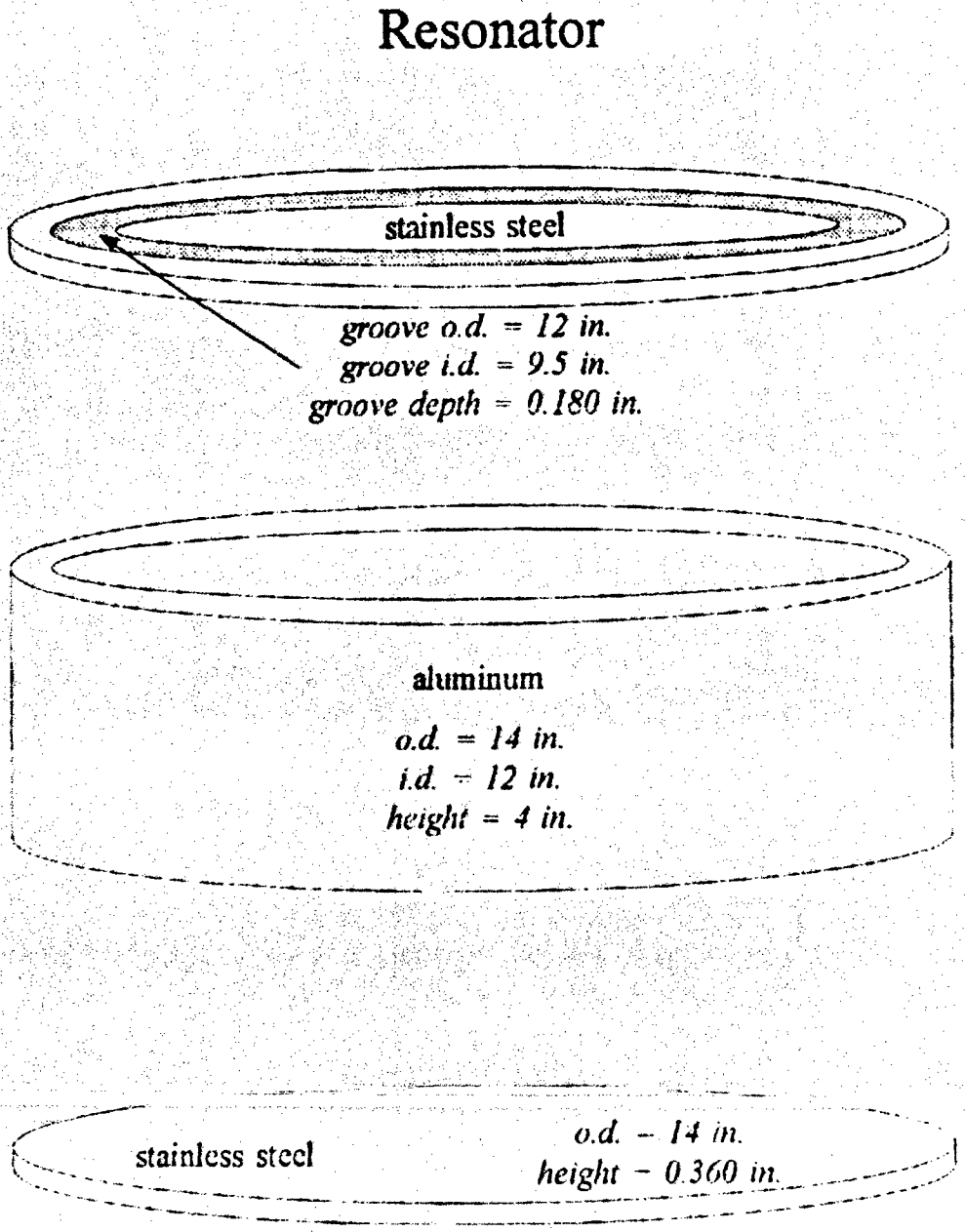

Figure 2: Radial engine resonator.

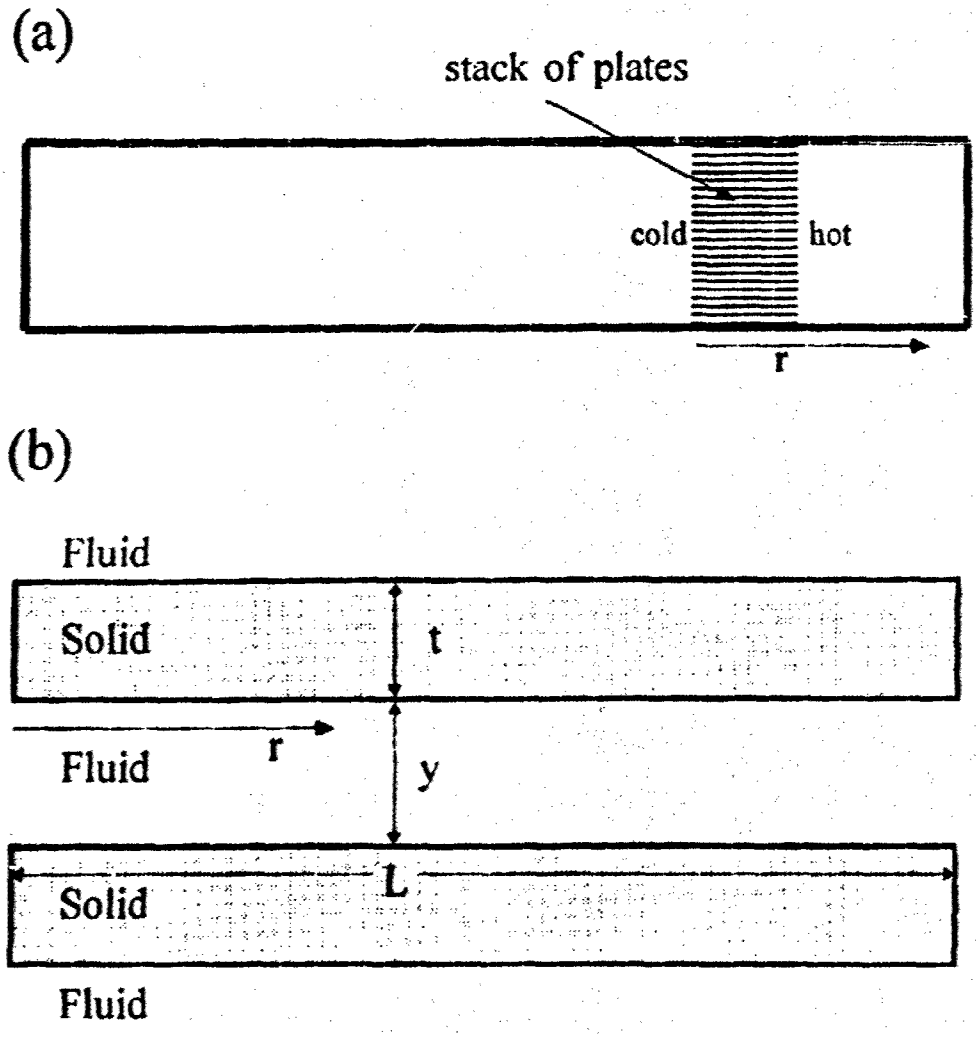

Figure 3: Parallel plate engine geometry. (a) Overall view, and (b) expanded view. Plates have thickness t, and fluid layers have thickness y.

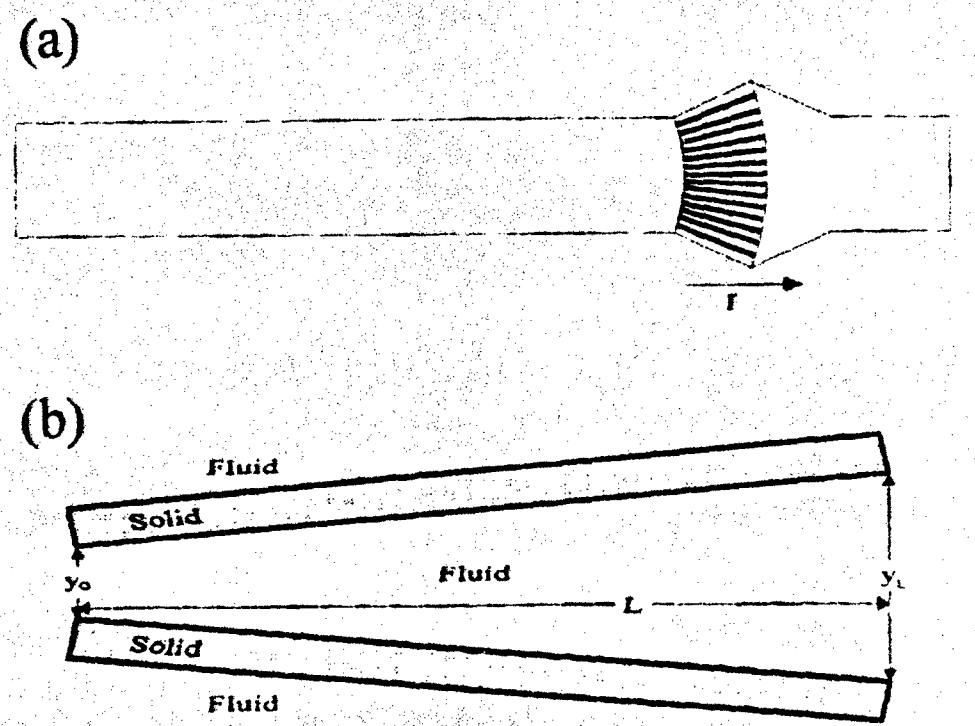

Figure 4: Sloped engine geometry. (a) Overall view, and (b) expanded view. Plates have thickness t, fluid layers have thickness $y(r)$, and y_0 is the fluid layer thickness at the left side of the stack.

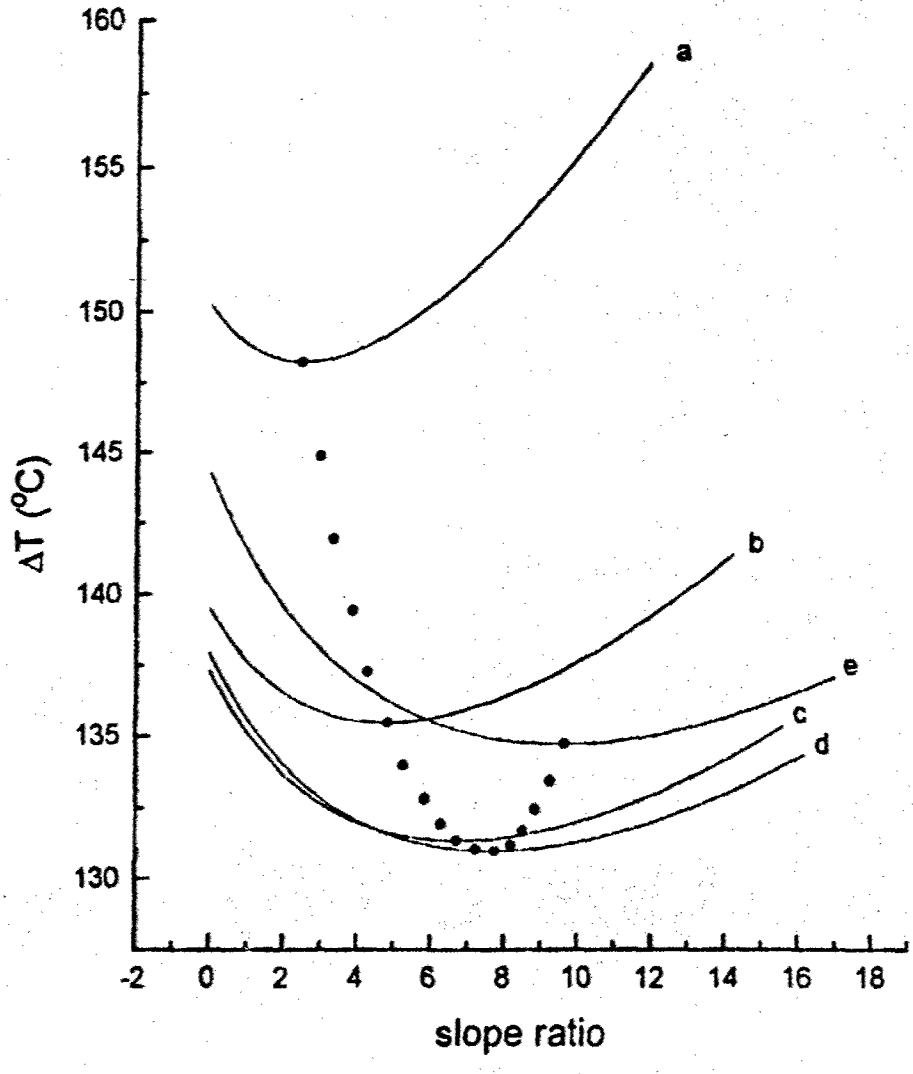

Figure 3. Quasi-temperature difference (ΔT) as a function of slope ratio. a) y_0 = 0.799 mm $\approx 2.266\delta_x$, b) $y_0 = 0.847$ mm, c) $y_0 = 0.919$ mm, d) $y_0 = 0.958$ mm, e) $y_0 = 1.065$ mm. Solid dots represent minima in ΔT for curves similar to a-e with different y_0 values. The ambient heat exchanger temperature is 293 K.

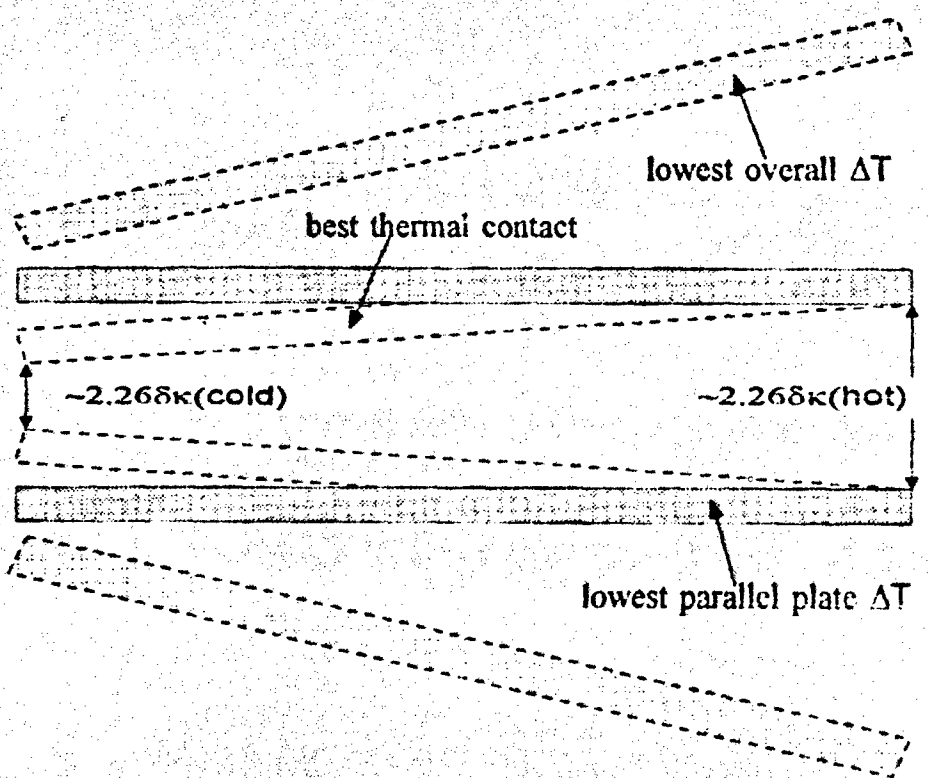

Figure 6: Simple visual representation of plate spacings which provide the lowest overall ΔT, the lowest parallel plate ΔT, and the best thermal contact between the fluid and the solid.

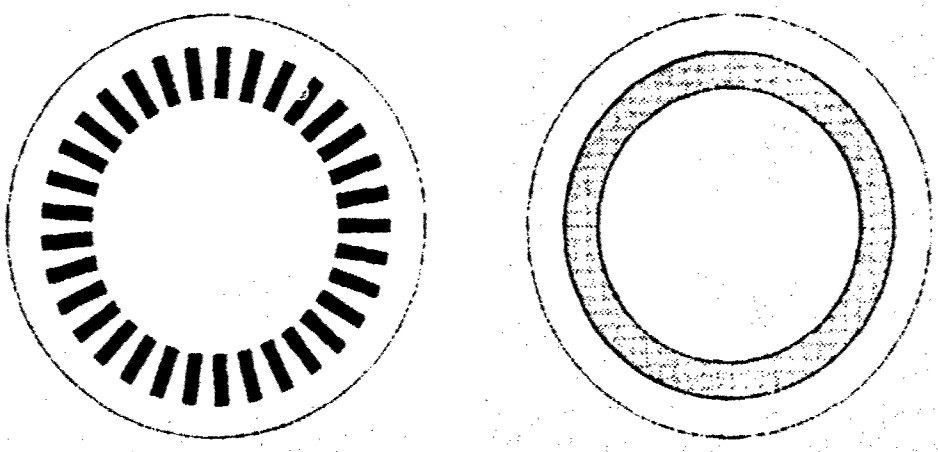

vertical stack

washer-style stack

Figure 7: Two different styles of radial engines. The vertical stack has a natural varying plate spacing, while the "washer" style stack is similar to the plane parallel plate stack since there is a constant plate spacing from one side to the other.

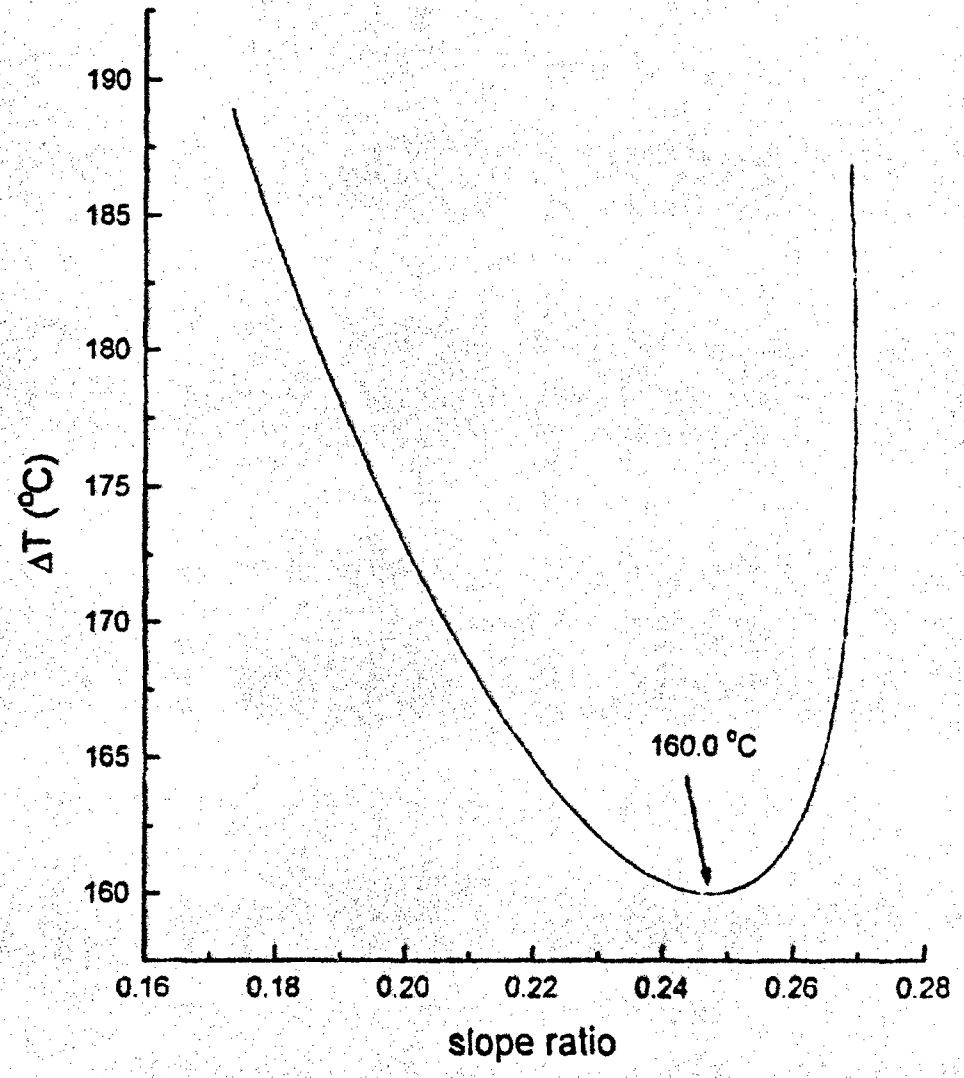

Figure 8: Onset temperature difference as a function of slope ratio for the [illegible] tical plate radial system. The lowest ΔT achieved by a similar "washer" style engine is 161.1 °C.

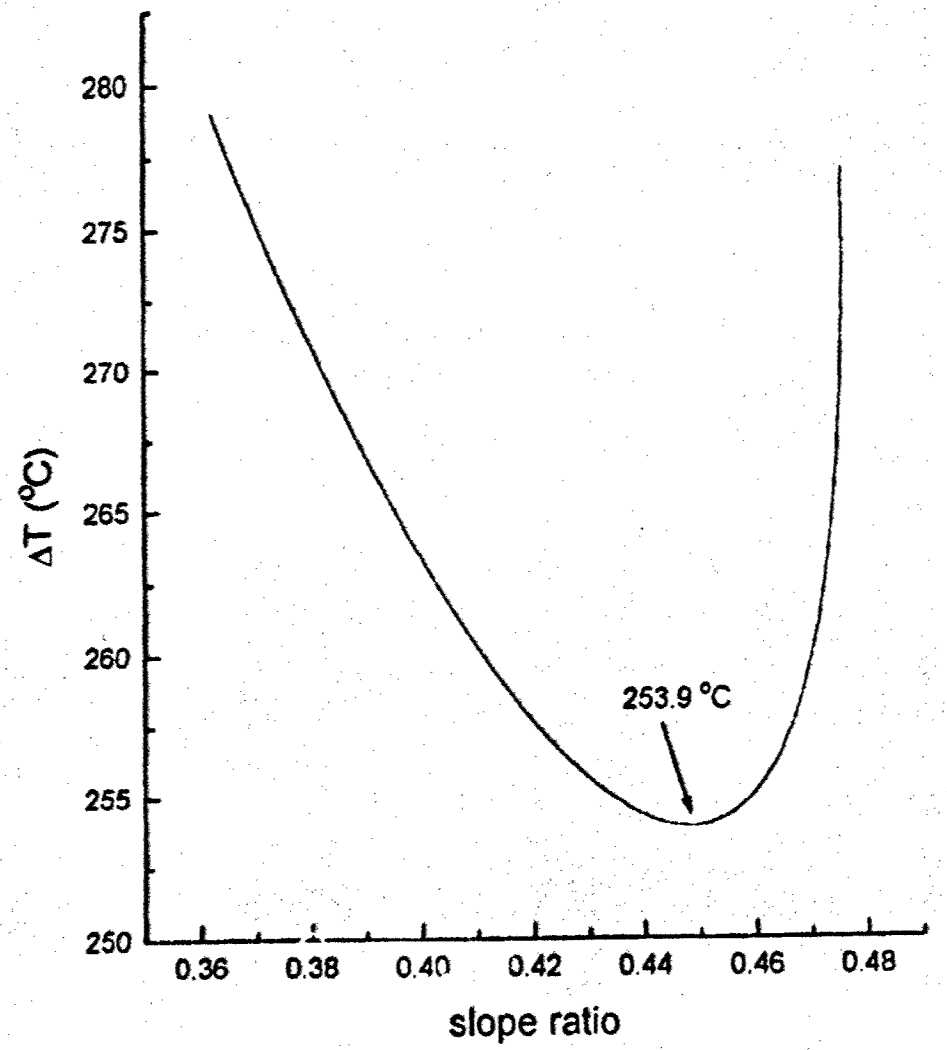

Figure 5. Power temperature difference as a function of slope ratio for the 1.47 KHz vertical plate radial system. The lowest ΔT achieved by a similar "washer" style engine is 255.4 $^{\circ}C$.

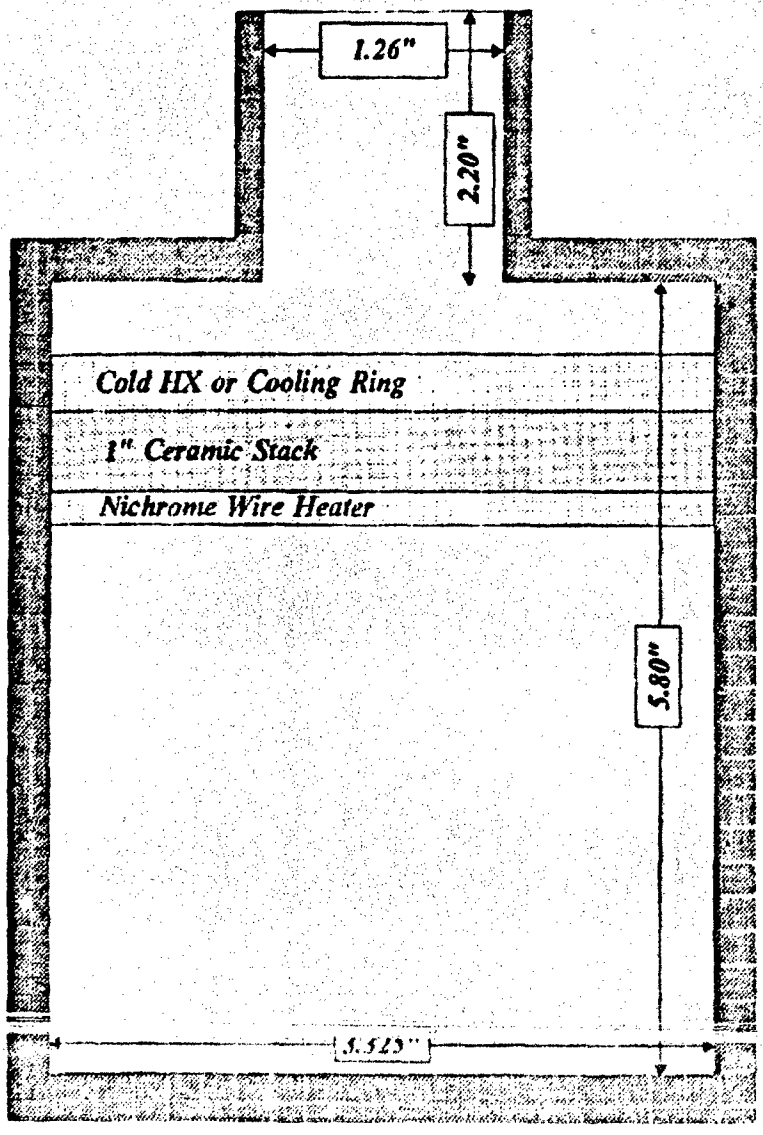

Figure 10: Thermoacoustically driven Helmholtz resonator.

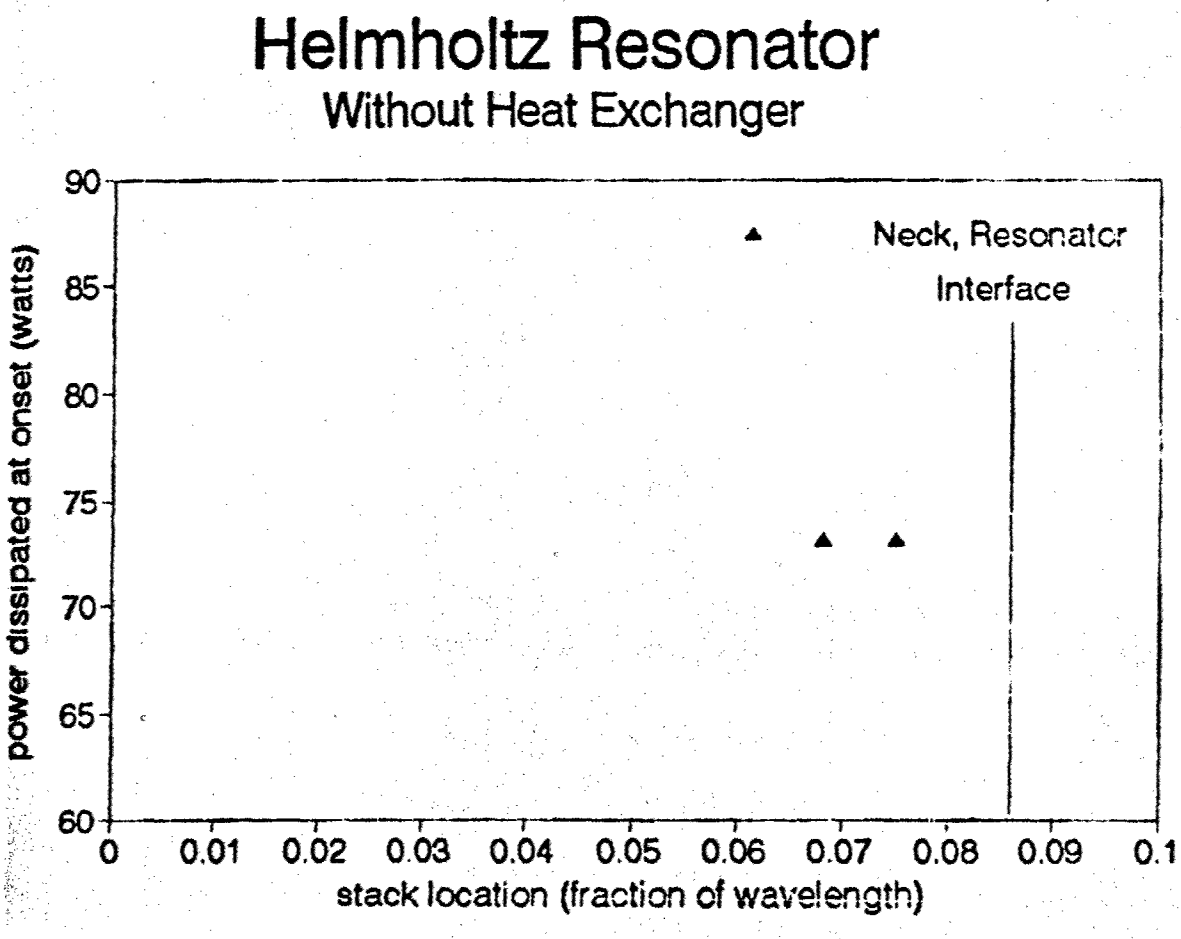

Figure 11: Power dissipated in nichrome wire heater at onset for different stack locations – with cooled open tube.

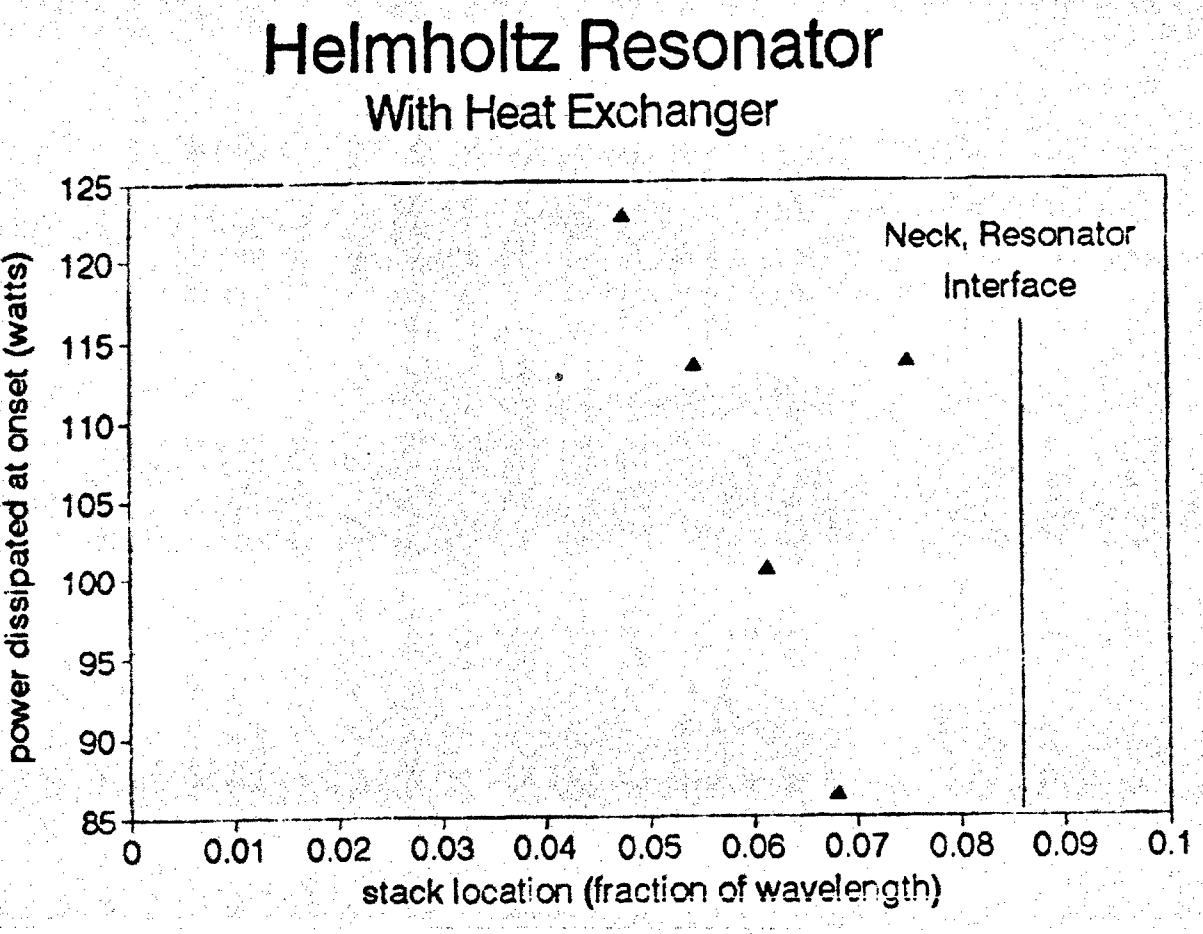

Figure 12. Power dissipated in nichrome wire heater at onset for different stack locations with cold heat exchanger.

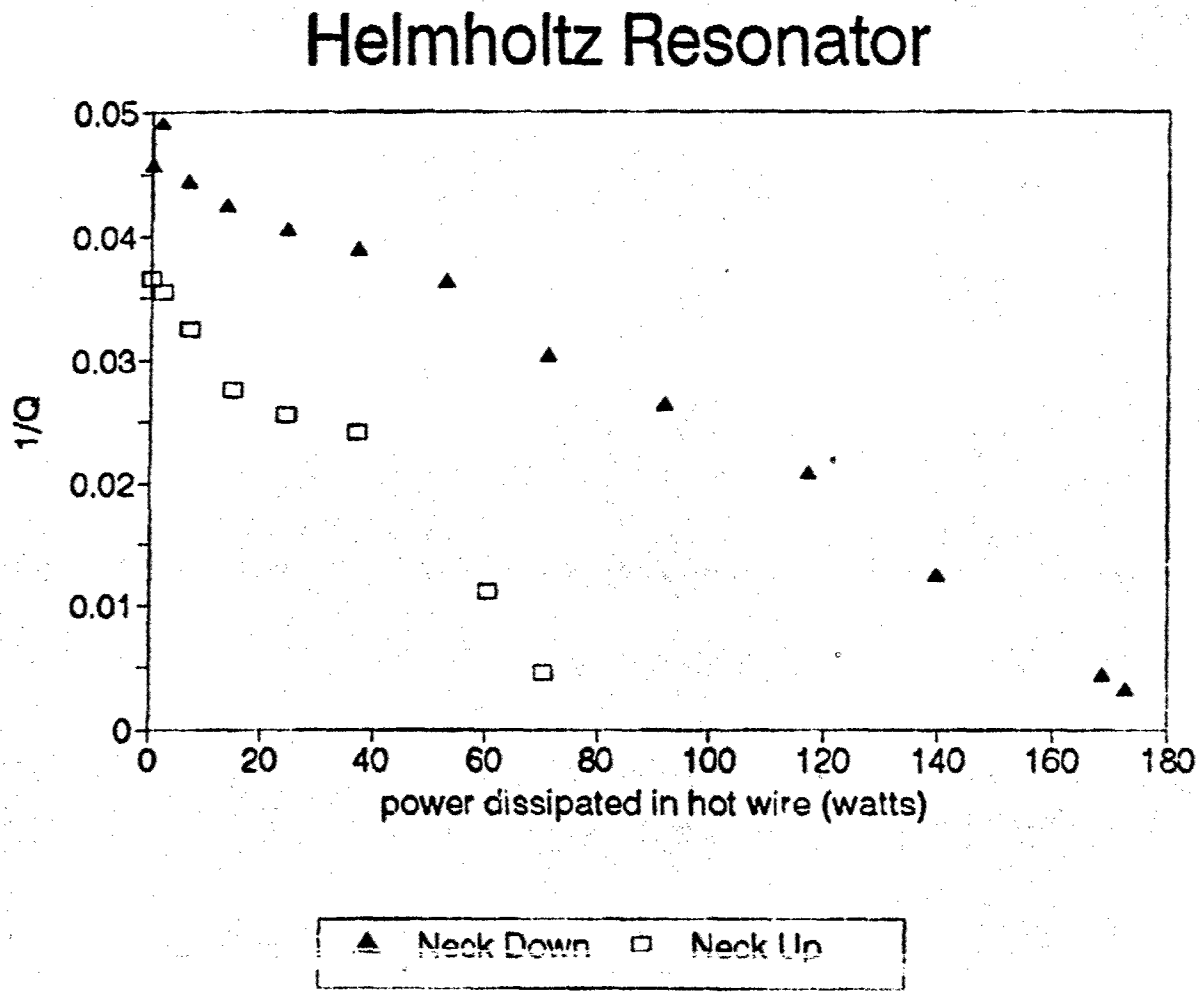

Figure 13: 1/Q as a function of the power dissipated in the nichrome wire for two different orientations of the resonator.

OFFICE OF NAVAL RESEARCH
PUBLICATIONS / PATENTS / PRESENTATIONS / HONORS REPORT
1 JUNE 1994 through 31 May 1995

R&T Number:	3126973ess01
Contract/Grant Number:	N00014-93-1-1125
Contract/Grant Title:	Experimental Studies of Radial Wave Thermoacoustic Engines
Principal Investigator:	Richard Raspet
Mailing Address:	National Center for Physical Acoustics The University of Mississippi University, MS 38677
Phone Number:	601-232-5808
E-Mail Address:	raspet@spare.ncpa.olemiss.edu

a. Number of Papers Submitted to Refereed Journal but not yet published: 1

b. Number of Papers Published in Refereed Journals: 0
(list attached)

c. Number of Books or Chapters Submitted but not yet Published:
0

d. Number of Books or Chapters Published: 0

e. Number of Printed Technical Reports & Non-Refereed Papers: 0

f. Number of Patents Filed: 0

g. Number of Patents Granted: 0

h. Number of Invited Presentations at Workshops or Prof. Society Meetings: 0

i. Number of Presentations at Workshops or Prof. Society Meetings:
3

j. Honors/Awards/Prizes for Contract/Grant Employees: 0

k. Total number of Graduate Students and Post-Docs Supported at least 25% this year on this Contract/Grant:

Grad Students 1 and Post-Docs 0 including

Grad Student Female 0 and Post-Docs Female 0

Grad Student Minority 0 and Post-Doc Minority 0

l. Total number of Undergraduates funded by this Contract/Grant for this reporting period:

OFFICE OF NAVAL RESEARCH
PUBLICATIONS / PATENTS / PRESENTATIONS / HONORS REPORT
1 JUNE 1994 through 31 May 1995

ATTACHMENTS

a. Papers Submitted to Refereed Journal

W. Patrick Arnott, Jay A. Lightfoot, Richard Raspet and Hans Moosmuller, "Radial Wave thermoacoustic engines: Theory and examples for refrigerators, prime movers, and high gain narrow bandwidth photoacoustic spectrometers," submitted to J. Acoust. Soc. Am., January 1995